NASA/CR—2002-211701

2002–GT–30213

Heat Transfer in a Complex Trailing Edge Passage for a High Pressure Turbine Blade

Part 2: Simulation Results

David L. Rigby
QSS Group, Inc., Cleveland, Ohio

Ronald S. Bunker
General Electric R&D Center, Schenectady, New York

August 2002

The NASA STI Program Office . . . in Profile

Since its founding, NASA has been dedicated to the advancement of aeronautics and space science. The NASA Scientific and Technical Information (STI) Program Office plays a key part in helping NASA maintain this important role.

The NASA STI Program Office is operated by Langley Research Center, the Lead Center for NASA's scientific and technical information. The NASA STI Program Office provides access to the NASA STI Database, the largest collection of aeronautical and space science STI in the world. The Program Office is also NASA's institutional mechanism for disseminating the results of its research and development activities. These results are published by NASA in the NASA STI Report Series, which includes the following report types:

- TECHNICAL PUBLICATION. Reports of completed research or a major significant phase of research that present the results of NASA programs and include extensive data or theoretical analysis. Includes compilations of significant scientific and technical data and information deemed to be of continuing reference value. NASA's counterpart of peer-reviewed formal professional papers but has less stringent limitations on manuscript length and extent of graphic presentations.

- TECHNICAL MEMORANDUM. Scientific and technical findings that are preliminary or of specialized interest, e.g., quick release reports, working papers, and bibliographies that contain minimal annotation. Does not contain extensive analysis.

- CONTRACTOR REPORT. Scientific and technical findings by NASA-sponsored contractors and grantees.

- CONFERENCE PUBLICATION. Collected papers from scientific and technical conferences, symposia, seminars, or other meetings sponsored or cosponsored by NASA.

- SPECIAL PUBLICATION. Scientific, technical, or historical information from NASA programs, projects, and missions, often concerned with subjects having substantial public interest.

- TECHNICAL TRANSLATION. English-language translations of foreign scientific and technical material pertinent to NASA's mission.

Specialized services that complement the STI Program Office's diverse offerings include creating custom thesauri, building customized data bases, organizing and publishing research results . . . even providing videos.

For more information about the NASA STI Program Office, see the following:

- Access the NASA STI Program Home Page at ***http://www.sti.nasa.gov***

- E-mail your question via the Internet to help@sti.nasa.gov

- Fax your question to the NASA Access Help Desk at 301–621–0134

- Telephone the NASA Access Help Desk at 301–621–0390

- Write to:
  NASA Access Help Desk
  NASA Center for AeroSpace Information
  7121 Standard Drive
  Hanover, MD 21076

NASA/CR—2002-211701 2002–GT–30213

Heat Transfer in a Complex Trailing Edge Passage for a High Pressure Turbine Blade

Part 2: Simulation Results

David L. Rigby
QSS Group, Inc., Cleveland, Ohio

Ronald S. Bunker
General Electric R&D Center, Schenectady, New York

Prepared for the
Turbo Expo 2002
cosponsored by the American Society of Mechanical Engineers
and the International Gas Turbine Institute
Amsterdam, The Netherlands, June 3–6, 2002

Prepared under Contract NAS3–00145

National Aeronautics and
Space Administration

Glenn Research Center

August 2002

Acknowledgments

The present work was supported by the NASA Glenn Research Center as part of the Coolant Flow Management Program. The authors wish to thank Mr. Steven Hippensteele and Dr. Raymond Gaugler, Chief of the Turbine Branch, for their support and encouragement of this work. Calculations were done on the NAS SGI clusters at the NASA Ames Research Center.

The Aerospace Propulsion and Power Program at NASA Glenn Research Center sponsored this work.

Available from

NASA Center for Aerospace Information
7121 Standard Drive
Hanover, MD 21076

National Technical Information Service
5285 Port Royal Road
Springfield, VA 22100

Available electronically at http://gltrs.grc.nasa.gov/GLTRS

Heat Transfer in a Complex Trailing Edge Passage for a High Pressure Turbine Blade Part 2: Simulation Results

David L. Rigby
QSS Group Inc.
Cleveland, Ohio 44135
Phone: 216-433-5965, Fax: 216-433-5802, Email: rigby@grc.nasa.gov

Ronald S. Bunker
General Electric R&D Center
Schenectady, New York 12301

ABSTRACT

A combined experimental and numerical study to investigate the heat transfer distribution in a complex blade trailing edge passage was conducted. The geometry consists of a two pass serpentine passage with taper toward the trailing edge, as well as from hub to tip. The upflow channel has an average aspect ratio of roughly 14:1, while the exit passage aspect ratio is about 5:1. The upflow channel is split in an interrupted way and is smooth on the trailing edge side of the split and turbulated on the other side. A turning vane is placed near the tip of the upflow channel. Reynolds numbers in the range of 31,000 to 61,000, based on inlet conditions were simulated numerically. The simulation was performed using the Glenn-HT code, a full three-dimensional Navier-Stokes solver using the Wilcox k-ω turbulence model. A structured multi-block grid is used with approximately 4.5 million cells, and average y+ values on the order of unity. Pressure and heat transfer distributions are presented with comparison to the experimental data. While there are some regions with discrepancies, in general the agreement is very good for both pressure and heat transfer.

NOMENCLATURE

A	Area of inlet
C_f	friction coefficient, $2\tau_w/\rho V^2$
D	inlet hydraulic diameter
h	heat transfer coefficient
k	thermal conductivity
$\dot{m}$	mass flow rate
Nu	Nusselt number, hD/k
P	pressure
Pr	Prandtl number
q_w''	Wall heat flux
Re	Reynolds number, VD/ν
T	Temperature
$T_{t,in}$	Total temperature at inlet
V	characteristic velocity, $\dot{m}/(\rho A)$
y^+	dimensionless distance from the wall, $\frac{\eta}{D} Re \sqrt{\frac{C_f}{2}}$
η	distance normal to wall
μ	viscosity
ρ	density
ν	kinematic viscosity

Subscripts

air	bulk condition
t	total condition
w	wall value

INTRODUCTION

The present work is motivated by the need to accurately predict heat transfer in turbomachinery. For efficient gas turbine operation, flow temperatures in the hot gas path exceed acceptable metal temperatures in many regions of the engine. To maintain the integrity of the parts for an acceptable engine life, they must be cooled. Efficient cooling schemes require accurate heat transfer prediction to minimize regions which are over-cooled, and even more importantly to ensure adequate cooling in high heat flux regions. With the advent of more powerful computers, three dimensional simulations of the internal coolant flow are becoming more common. The Glenn-HT code is a Reynolds averaged Navier-Stokes solver which has proven to be

an accurate and robust simulation tool for flowfield and heat transfer prediction. Many papers have been published demonstrating the use of the code on many configurations. Some recent configurations include turbine rotors with clearance (Ameri and Bunker [1], Ameri and Rigby [2]), internal/external flow coupled through cooling holes (Heidemann et al. [3], Garg and Rigby [4]), and rotating internal passages with ribs (Rigby [5]). Additionally, simulations have been performed which include internal and external flows coupled through a conjugate solution of the solid region (Rigby and Lepicovsky [6])

Traditional cooling passage analysis relies heavily on empirical data bases and quasi-one-dimensional techniques. Higher fidelity prediction capabilities are needed to allow attempts at more advanced and novel configurations. The capabilities of the current computers make it possible to simulate reasonably complex geometries, such as the one in the present study. Beyond obtaining the required computing resources, there are two additional major issues. As we turn our attention to more complex geometries, the two additional issues are grid generation and turbulence modeling.

The present work was undertaken in an attempt to assess our abilities in grid generation and to test the turbulence model on increasingly complex geometries. The present geometry includes variation in channel shape and size in the flow direction. Also, turbulated regions are combined with smooth regions such that there are several areas where turbulators do not end at a side wall. A final complication arises from the interrupted nature of the split upflow channel, which has turbulators to one side and smooth region on the other side. Three basics questions were to be answered in this undertaking: First could a structured multi-block grid be generated, second would the code run to convergence on what had to be a less than ideal grid, and third would the simulation agree with the experimental data? The answer on all three counts is yes. The commercially available grid generation software, ICEMCFD, proved to be quite capable of generating a reasonable grid. The Glenn-HT code also proved to be robust and produced results which agree very well with the data.

NUMERICAL PROCEDURE

Brief description of Glenn-HT code

The simulations performed in this study were done using a computer code currently called Glenn-HT. In the past the code was named TRAF3D.MB (Steinthorsson et al. [7]). This code is a general purpose flow solver, designed for simulations of flows in complicated geometries. The code is based on the TRAF3D code, an efficient computer code designed for simulations of flows in turbine cascades (Arnone et al. [8]). The Glenn-HT code employs the full compressible Navier-Stokes equations. It uses a multi-stage Runge-Kutta scheme to march in pseudo time. For convergence acceleration the code uses, among other techniques, local time stepping. The spatial variation in the time step takes into account both convective and diffusive stability limits. In addition, the code utilizes multi-grid and implicit residual smoothing to accelerate convergence to steady state. Convective and diffusive fluxes are computed using central differencing. Artificial dissipation is added to prevent odd-even decoupling. The discretization is formally second order accurate. To handle complex geometries, the code uses contiguous structured multi-block grid systems but has the added capability of handling grids with non-contiguous grid lines across branch cuts. For contiguous systems, all internal boundaries are conservative. The TRAF3D.MB code was described in detail by Steinthorsson et al. [7]. Some aspects of the formulation used in the code are the same as those described by Arnone et al. [8]. The code is fitted with the low Reynolds number k-ω turbulence model of Wilcox [9].

DESCRIPTION OF GEOMETRY AND CONDITIONS

Figures 1 and 2 show a schematic of the test model. Figure 1 shows the bottom surface which is flat. The two main passages are seperated by a continuous 3.18 mm rib. The inlet passage is divided by an interupted 3.18 mm rib, allowing flow to pass between 1A and 1B. A turning vane is located in the trailing edge tip corner. As shown in figure 2, the upper surface slopes from passage 2 to the trailing edge. In addition, the upper surface slopes from the root to the tip. All turbulators are square in cross-section and angled at 45 degrees. In passage 1B the turbulators near the inlet are 2.03 mm high, while the seven nearsest the tip are 1.52 mm high. In passage 2, the six turbulators nearest the tip are 1.52 mm high, with the remainder being 2.54 mm high. In general, the ratio of turbulators spacing to height is 10. On the upper surface, the turbulators are staggered relative to the lower surface.

In the experiment, an inlet plenum is used for passage 1. For the numerical calculation an additional 7.62 cm was added so there would be no turbulators at the inlet or exit. Without this extension, it is expected that there would have been problems with boundary conditions and robustness. Since heat transfer data is not collected until well into the test section, an acceptable match in the measurement region was expected.

Figure 3 shows a perspective view of the geometry. The bottom flat wall is shown in gray and the black lines show the outlines of grid blocks. Flow enters through passages 1A and 1B, and exits through passage 2. From figure 3 it can be seen that the passages are trapezoidal in cross section and are thickest near passage 2 and thinnest near passage 1A, the trailing edge. In addition, the passages thin as the tip is approached. In figure 3, the location x=0 is where the experimental test section began.

Figure 4 shows the bottom wall grid in the region which is heated. The interrupted nature of the split between 1A and 1B, and the turning vane are visible in figure 4. Also, it can be seen that passage 1A is smooth, while 1B and 2 have turbulators at a 45 degree angle. The upper wall looks much the same as the bottom, with the turbulators at the same angle and staggered

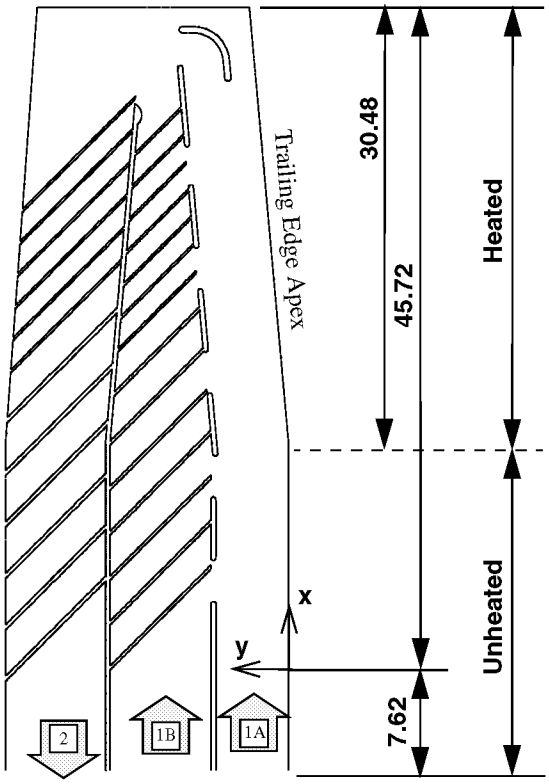

Figure 1. Schematic of flat lower surface. (dimensions in centimeters)

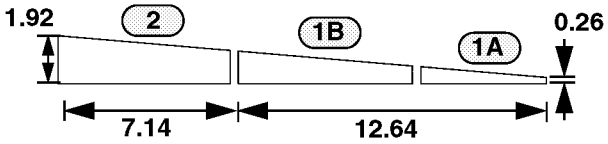

Figure 2. Schematic of Inlet Cross-Section. (dimensions in centimeters)

relative to those on the bottom wall. Additional details on the geometry are provided in Part 1 of this work (Bunker et al. [10]).

Three flow conditions were run numerically. In each case the exit pressure was the same and the wall temperature in the heated region was maintained at 1.1 times the inlet total temperature. The average inlet total pressure for each of the three cases was 1.28, 1.46, and 1.81 times the exit static pressure. The total pressure imposed on passage 1A was slightly less than that on passage 1B as was observed in the experiment. The resulting Reynolds numbers based on inlet conditions for the Low, Medium and High pressure ratios were 31,000, 43,000, and 61,000, respectively. The inlet hydraulic diameter is based on the combination of both 1A and 1B.

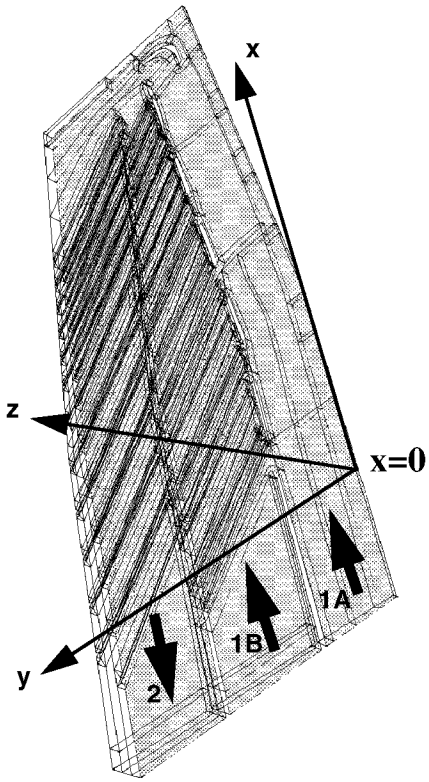

Figure 3. Perspective view of geometry including block boundaries.

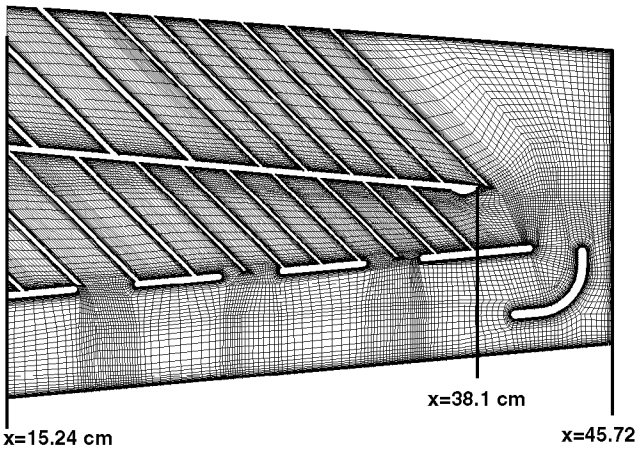

Figure 4. Grid on heated region.

Each case took approximately 1000 cpu hours on a SGI Origin cluster. Most runs were done with 32 processors in parallel resulting in running times on the order of 30 hours. This case ran effeciently even at 95 processors, the largest number attempted. However, due to the shared nature of the machine, a request for 95 processors resulted in a very long wait in the queue.

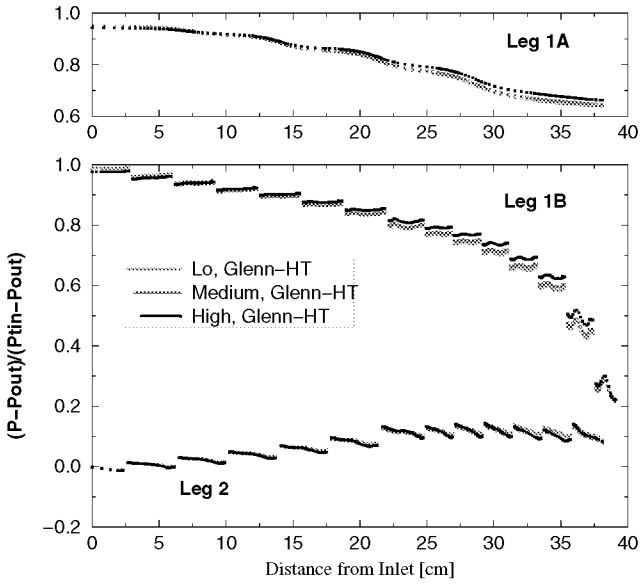

Figure 5. Normalized pressure down center of each channel.

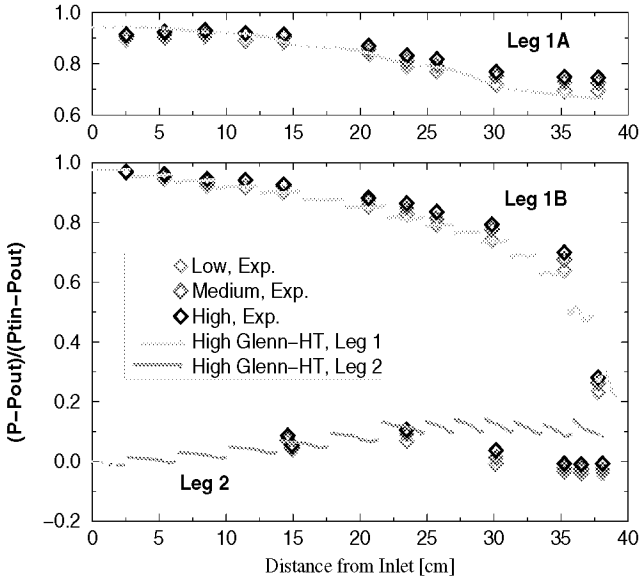

Figure 6. Normalized pressure down center of each channel with experimental data.

RESULTS

Pressure

Figure 5 shows the pressure distribution down the center of each of the passages, for the three different pressure ratios. The results for channel 1A are provided above the figure for clarity, since they are nearly equal to those in channel 1B. The first thing apparent from figure 5 is that the pressure distributions are very similar for each case. The pressures in channel 1A fall smoothly in the flow direction closely matching the drop in channel 1B. In channel 1B the pressure is fairly uniform between turbulators with jumps across the turbulator. The rapid drop in pressure near the end of channel 1B occurs because of the rapid acceleration of the flow through the reduced area. channel 2 shows similar jumps in pressure across the turbulators to those in channel 1B, along with significant adverse pressure gradient between the turbulators.

Figure 6 is similar to figure 5, except the experimental results are included and only the high pressure ratio for the Glenn-HT case is shown. It is apparent that comparison with the experiment is very good with the exception of the region of channel 2 near the tip. In that region, which is the turn and recovery region, the experimental pressures fall well below the prediction as well as below the exit pressure. As shown in the next section, the turn and recovery region is associated with a discrepency in heat transfer results between CFD and the experiment. The pressures in channel 1A and 1B compare quite well with the simulation matching the rate of drop as well as the rapid drop in channel 1B near the tip. Pressures in the middle of channel 2 also match well.

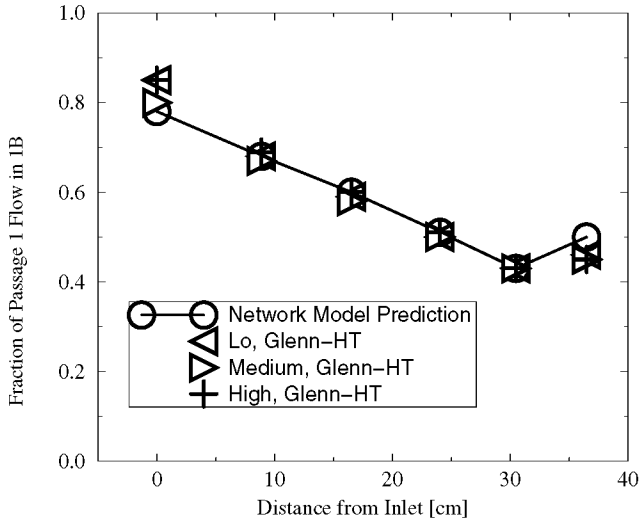

Figure 7. Fraction of passage 1 mass flow in 1B.

In Part 1 of this work the results of a one-dimensional, multi-element flow model were used to estimate the flow split between passages 1A and 1B. Those results are shown in figure 7 along with the results from the Glenn-HT simulation. The agreement of the Glenn-HT simulation with the Network Model is very good. These results also indicate that the flow split is essentially independent of Reynolds number.

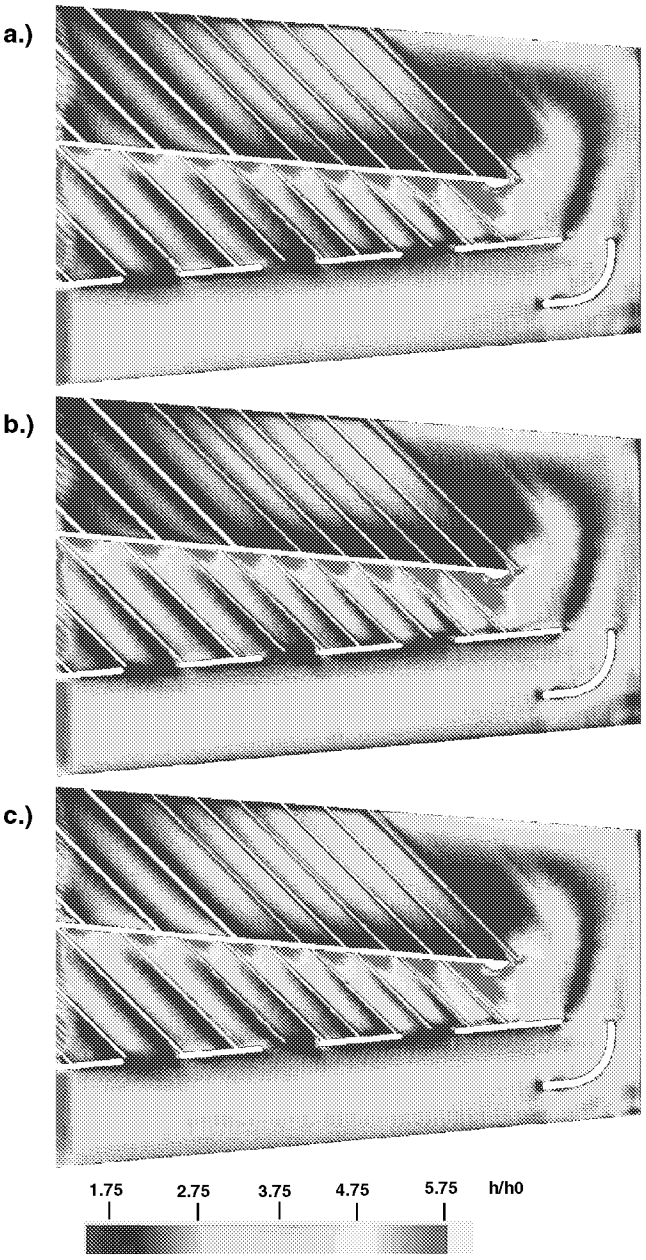

Figure 8. Normalized heat transfer coefficient for Low(a), Medium(b), and High(c) pressure ratio simulations.

Heat Transfer

Heat transfer results are presented in terms of the heat transfer coefficient defined by

$$h = \frac{q_w''}{(T_w - T_{air})} \tag{1}$$

where T_{air} is the average between inlet and exit total temperatures, which should produce essentially the same value for T_{air} as used in the experiment. For turbulent flows, it is generally expected that the heat transfer coefficient will vary nearly like the Reynolds number to the 0.8 power. In light of that expectation the results for the different cases are presented in normalized form. The heat transfer coefficient for each case is normalized by the value predicted by the Dittus-Boelter correlation based on the Reynolds number at the inlet to passage 1. The Dittus-Boelter correlation

$$h_0 = 0.023\left(\frac{k}{D}\right)Re_D^{0.8}Pr^{0.4} \tag{2}$$

predicts the heat transfer coefficient for a smooth pipe with fully developed turbulent flow.

Figure 8 shows the normalized heat transfer coefficient for the Low, Medium and High pressure ratio simulations. The purpose of showing this figure first is to simply show that, when normalized, the cases are nearly identical. The cases differ significantly in Reynolds number, doubling between the Low and High pressure ratios, and yet the match is nearly perfect. So the code is definitely producing a dependence on Reynolds number to the 0.8 power as was observed in the experimental results presented in Part 1 of this work.

Figure 9 shows the normalized heat transfer coefficient for the experiment at the high pressure ratio. The color bar is labeled for both normalized and dimensional [W/m^{2}K] heat transfer coefficient. Since the colors are chosen to match between the CFD and experimental figures, one can now compare the experimental results in figure 9 to the numerical results in figure 8. The white

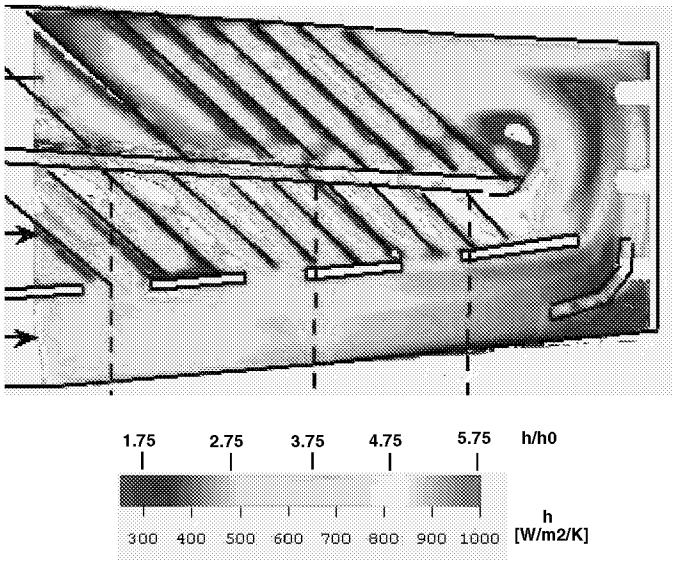

Figure 9. Normalized heat transfer coefficient for High Pressure Ratio experiment. (color bar also shows dimensional value.

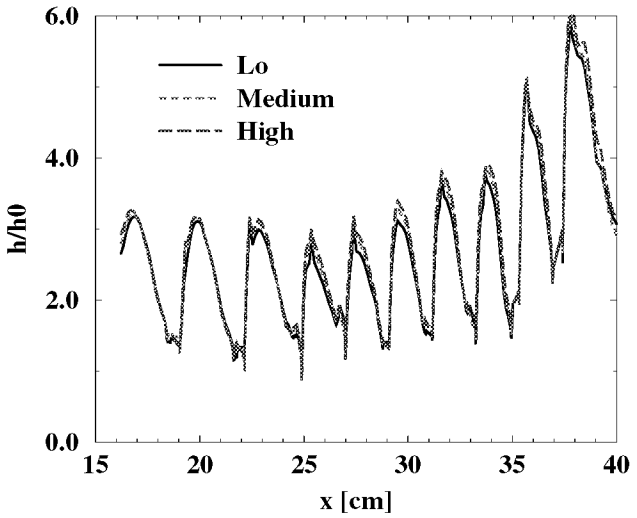

Figure 10. Normalized heat transfer coefficient on a line down the middle of passage 1B.

regions in the experimental figure are where data was not obtained, due to temperature limitations of the model materials. Qualitatively, the comparison is very good. High heat transfer is observed between the turbulators, as expected. In addition, the low streak emanating from the tip of the split between passages 1A and 1B is closely matched. Very high values after the final rib in passage 1B, as well as the low region around the tip of the split between passages 1B and 2, are visible in both experiment and simulation. Although, the simulation produces a much larger low heat transfer region at the entrance to passage 2. The rise in heat transfer on the outer wall of passage 2 shown in the experiment is also predicted by the simulation. The level of increase in heat transfer between the turbulators is generally underpredicted by the simulation. The level in the smooth passage, 1A, is predicted closely by the simulation.

In figure 10, the normalized heat transfer coefficient on a line down the middle of passage 1B is shown for the Low, Medium and High pressure ratio cases. One can now see, in a quantitative way, the similarity between the solutions. The average of each of the lines in figure 10 are each within ±5% and the maximum diference is <10%.

Figure 11 shows the same result as figures 8c and 9, except the scaling is changed to highlight the features in the tip region. In this figure, once again the features are quite similar. The low streak emanating from the splitter between 1A and 1B, along with the high streak wrapping around the tip of the splitter between 1B and 2. A high heat transfer region exists at the end of the turning vane for both experiment and simulation. Although, in the experiment the high region seems to be aligned with the turning vane, while in the simulation it occurs more toward the inside of the turn. One additional discrepancy is noted in the region to the outside of the turning vane, the very low experimental values are not present in the simulation.

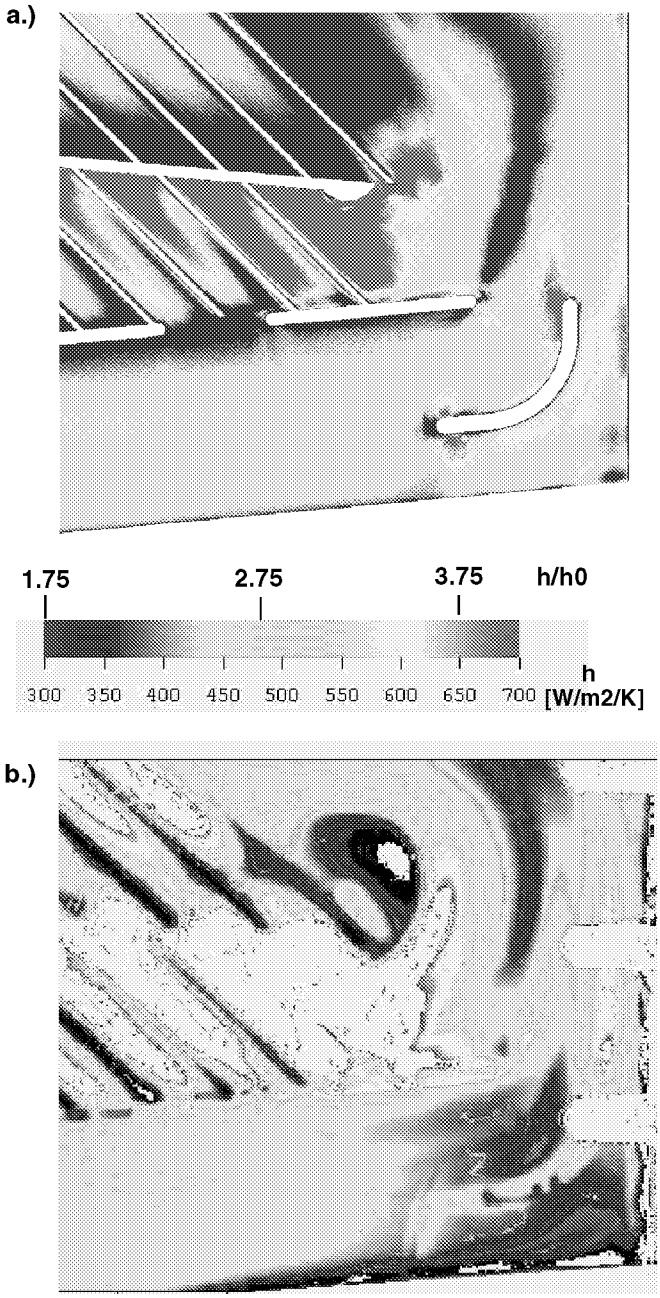

Figure 11. Normalized heat transfer coefficient for high pressure ratio simulation(a) and experiment(b) scaled to show turn.

Figure 12 shows results for the low pressure ratio case. All of the features and the level of comparison are the same as for the high pressure ratio.

An observant reader may have noticed that block boundaries are visible in some regions of the heat transfer figures. For

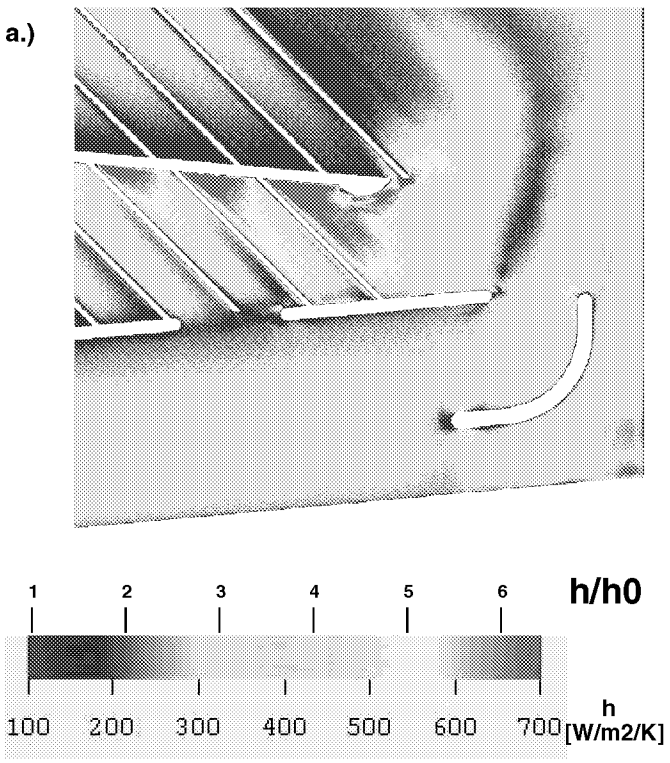

Figure 12. Normalized heat transfer coefficient for low pressure ratio simulation(a) and experiment(b) scaled to show turn.

instance, figure 11a near the turning vane. These are merely artifacts of less than perfect post-processing. The solution is produced on cell centers. The heat transfer is then calculated on face centers and interpolated to the grid nodes. Because of these

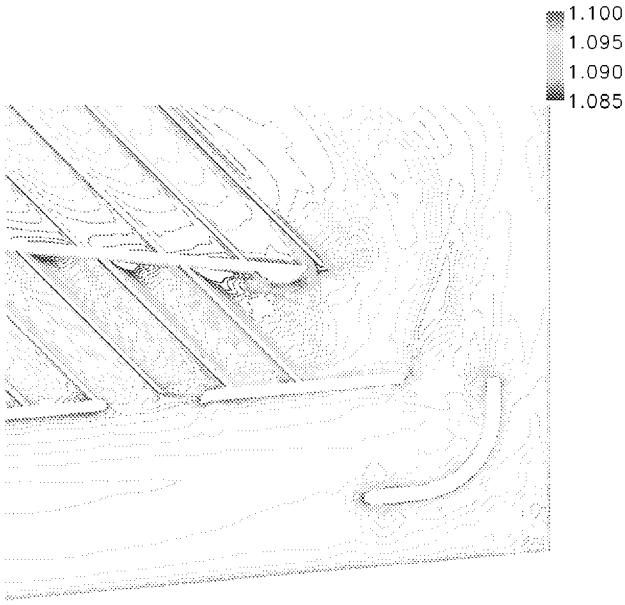

Figure 13. Temperature normalized by inlet total temperature. Cut plane is located one grid space off wall.

manipulations, a little bit of "noise" is to be expected. Figure 13 is offered as further evidence of the high quality of the codes block handling ability. Figure 13 shows the temperature distribution one grid space off the wall. From figure 13 it can be seen that the temperature is continuous and smooth across block boundaries.

One benefit of running a simulation is the ability to investigate the flow field everywhere in the domain, which can in turn allow further insight into why things appear as they do. Figure 14 shows the velocity component normal to the heated wall. The plane shown is located above the wall at a height equal to the height of the ribs in the tip region. No scale is shown for figure 14, since its purpose is to highlight the sign of the normal velocity component. Figure 14 bears a striking resemblance to figure 8, with the colors reversed. In general, regions of high heat transfer coincide with regions of flow toward the surface. Notice that between the turbulators in passage 1B there is a region of down flow just after the turbulator, followed by a region of upflow just upstream of the turbulator. From figure 8 we see that the highest heat transfer between turbulators in passage 1B tends to be just downstream of the rib where the flow at rib height is toward the surface. In passage 2, which has significantly less blockage compared to passage 1B, the normal velocity at rib height is toward the wall over much of the region between turbulators. Referring to figure 8 again we see that the predominantly downward flow between the passage 2 turbulators leads to a heat transfer distribution which is not skewed toward the upstream turbulator. In the turn region we see a strong upwelling of flow associated with the low

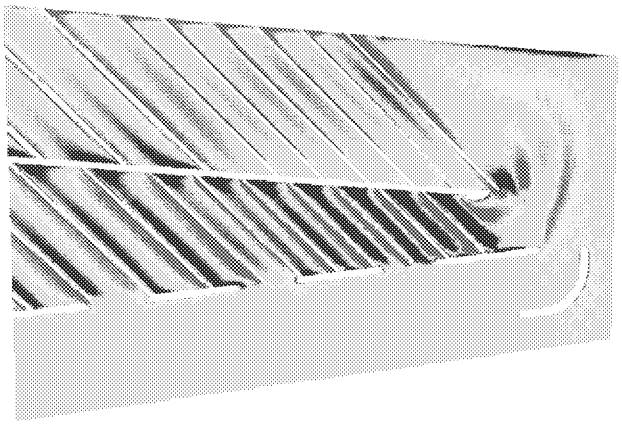

Figure 14. Velocity component normal to surface. Cut plane is located at the height of the turbulators near the tip. (Red is away and blue is toward surface)

heat transfer streak emanating from the splitter between passages 1A and 1B. Also, a downward flow is associated with the high heat transfer on the outer wall of passage 2. One final observation on figure 14 is that flow away from the surface does not always imply low heat transfer. Looking at the end of passage 1B, where the area becomes quite small, figure 14 shows a strong upwelling of flow. However, figure 8 shows high heat transfer in this area. This reversal of the general trend is of course due to the tremendous streamwise acceleration occurring as the flow exits passage 2.

CONCLUSIONS

A simulation of flow and heat transfer in a complex trailing edge passage for a high pressure turbine blade was done using the Glenn-HT Navier-Stokes code. The geometry attempted represents the most complex internal passage attempted with this code to date. The code proved to be very robust even though the grid was highly nonorthogonal and somewhat nonsmooth in places. Results of the pressure and heat transfer distributions compare very well with the available experimental data, with the exception of some localized discrepenancies. The dependence of heat transfer on Reynolds number to the 0.8 power observed in the experiment, was reproduced by the simulation very closely. The availability of the simulation allows in depth investigation of flow features and their effect on heat transfer.

REFERENCES

[1] Ameri, Ali and Bunker, R.S., "Heat Transfer and Flow on the First-Stage Blade of a Power Generation Gas Turbine: Part 2-Simulation Results," ASME J. Turbomach., 122 pp 272-277, 2000.

[2] Ameri, Ali and Rigby, D.L., "A Numerical Analysis of the Heat Transfer and Effectiveness on the Film Cooled Turbine Blade Tip Models," 4th Int. Sym. on Air Breathing Engines, Florence, Italy, 1999.

[3] Heidmann, J.D., Rigby, D.L., and Ameri, Ali, "A Three-Dimensional Coupled Internal/External Simulation of a Film-Cooled Turbine Vane," IGTI paper 99-GT-, 1999.

[4] Garg, V.K. and Rigby, D.L., "Heat Transfer on a Film-Cooled Blade - Effect of Hole Physics," Int. J. of Heat and Fluid Flow, Vol. 20, pp. 10-25, 1999.

[5] Rigby, D.L., "Prediction of Heat and Mass Transfer in a Rotating Ribbed Coolant Passage with a 180 Degree Turn," IGTI paper 98-GT-329, 1998.

[6] Rigby, D.L. and Lepicovsky, J., "Conjugate Heat Transfer Analysis of Internally Cooled Configurations," IGTI Paper 2001-GT-405, 2001.

[7] Steinthorsson, E., Liou, M.S., Povinelli, L.A., "Development of an Explicit Multiblock/Multigrid Flow Solver for Viscous Flows in Complex Geometries," AIAA-93-2380, 1993.

[8] Arnone, A., Liou, M.-S., and Povinelli, L. A.,1991, "Multigrid Calculation of Three-Dimensional Viscous Cascade Flows," AIAA-91-3238.

[9] Wilcox, D.C., 1994b,"Simulation of Transition with a Two-Equation Turbulence Model," AIAA Journal, Vol. 32, No.2, pp. 247-255.

[10] Bunker, R.S., Wetzel, T.G. and Rigby, D.L., "Heat Transfer in a Complex Trailing Edge Passage for a High Pressure Turbine Blade- Part 1: Experimental Measurements," IGTI Paper 2002-GT-30212, 2002.

REPORT DOCUMENTATION PAGE

Form Approved
OMB No. 0704-0188

1. AGENCY USE ONLY (*Leave blank*)	2. REPORT DATE	3. REPORT TYPE AND DATES COVERED
	August 2002	Final Contractor Report

4. TITLE AND SUBTITLE

Heat Transfer in a Complex Trailing Edge Passage for a High Pressure Turbine Blade

Part 2: Simulation Results

5. FUNDING NUMBERS

WU–708–28–13–00
NAS3–00145

6. AUTHOR(S)

David L. Rigby and Ronald S. Bunker

7. PERFORMING ORGANIZATION NAME(S) AND ADDRESS(ES)

QSS Group, Inc.
21000 Brookpark Road
Cleveland, Ohio 44135

8. PERFORMING ORGANIZATION REPORT NUMBER

E–13430

9. SPONSORING/MONITORING AGENCY NAME(S) AND ADDRESS(ES)

National Aeronautics and Space Administration
Washington, DC 20546–0001

10. SPONSORING/MONITORING AGENCY REPORT NUMBER

NASA CR—2002-211701
2002–GT–30213

11. SUPPLEMENTARY NOTES

Prepared for the Turbo Expo 2002 cosponsored by the American Society of Mechanical Engineers and the International Gas Turbine Institute, Amsterdam, The Netherlands, June 3–6, 2002. David L. Rigby, QSS Group, Inc., Cleveland, Ohio 44135; and Ronald S. Bunker, General Electric R&D Center, Schenectady, New York 12301. Project Manager, Stephen Hippensteele, Turbomachinery and Propulsion Systems Division, NASA Glenn Research Center, organization code 5820, 216–433–5897.

12a. DISTRIBUTION/AVAILABILITY STATEMENT

Unclassified - Unlimited
Subject Categories: 07 and 34 Distribution: Nonstandard

Available electronically at http://gltrs.grc.nasa.gov/GLTRS

This publication is available from the NASA Center for AeroSpace Information, 301–621–0390.

12b. DISTRIBUTION CODE

13. ABSTRACT ***(Maximum 200 words)***

A combined experimental and numerical study to investigate the heat transfer distribution in a complex blade trailing edge passage was conducted. The geometry consists of a two pass serpentine passage with taper toward the trailing edge, as well as from hub to tip. The upflow channel has an average aspect ratio of roughly 14:1, while the exit passage aspect ratio is about 5:1. The upflow channel is split in an interrupted way and is smooth on the trailing edge side of the split and turbulated on the other side. A turning vane is placed near the tip of the upflow channel. Reynolds numbers in the range of 31,000 to 61,000, based on inlet conditions, were simulated numerically. The simulation was performed using the Glenn-HT code, a full three-dimensional Navier-Stokes solver using the Wilcox k-ω turbulence model. A structured multi-block grid is used with approximately 4.5 million cells and average y+ values on the order of unity. Pressure and heat transfer distributions are presented with comparison to the experimental data. While there are some regions with discrepancies, in general the agreement is very good for both pressure and heat transfer.

14. SUBJECT TERMS

Heat transfer; Turbine; Cooling; CFD

15. NUMBER OF PAGES

14

16. PRICE CODE

17. SECURITY CLASSIFICATION OF REPORT	18. SECURITY CLASSIFICATION OF THIS PAGE	19. SECURITY CLASSIFICATION OF ABSTRACT	20. LIMITATION OF ABSTRACT
Unclassified	Unclassified	Unclassified	